Inspection and Evaluation of Concrete Pagoda Structure by Non-Destructive Testing

Pathawee Sombat[1]*, Saharat Buddhwanna[2], Suporn Wilasri[3] and Sarouch Silakarn[4]

[1,2,3] Department of Civil Engineering, Faculty of Engineering at Thammasat University, Pathum Thani, THAILAND
[4] Department of Civil Engineering, Faculty of Architectural at Thammasat University, Pathum Thani, THAILAND

E-mail address: pathawee.som@dome.tu.ac.th, bsaharat@engr.tu.ac.th, Linesupornwilasri@gmail.com, sarouch1969@gmail.com

Abstract

Non-destructive testing (NDT) is a reliable method for determining the structural integrity of new and old construction and understanding the conditions of structural defects. It has been acknowledged that the interpretation of non-destructive evaluation has a significant impact on the reliability and consistency of the operator's knowledge and expertise. Within this era, there has been numerous research and articles upon the topic of Non-Destructive Evaluation (NDE); to refine the methodologies or to innovate the existing tools in order for NDTs to be used in onsite inspection more frequently. In this paper particularly, we were inquired for evaluating and analyzing the integrity of a pagoda, resistance to loads as well as its true dimensions, located in a temple named "Putha-Jedi" in Kanjanadhit sub-district, Surat Thani district, Thailand, by using the methods of NDT such as Schmidt hammer test, and Ferro scan technique. The parameters acquired will be used for redesigning or strengthening that pagoda.

Keywords: ("NDT", "NDE", "Structural Evaluation", "RC structures", "Structural loads and resistances")

Introduction

This project emphasized using Non-Destructive Evaluation on concrete structures to investigate the mechanical properties of those structures in which the structure that will be evaluated is a pagoda located in the southern part of Thailand, Surat Thani province, in the temple named "Putha-Jedi". The pagoda was built by the locals who are not specialized in civil engineering but rather the local wisdom of constructing pagoda that was passed down from the previous builder. Once it was noticed by the experts, the construction phase was then paused. The pagoda already consists of footing foundations, columns, beams and an outer layer of masonry wall with concrete plaster. Here is where NDE plays a key role, as we want to know how much the pagoda can resist the loads and will it need for re-design.

1. Background

1.1 Putha-jedi

A pagoda in the Putha-Jedi temple was built since 2017 as an abbot was asked by the locals' residents, whom donate their money to help rehabilitate the temple, to build a pagoda as a request, so they employed a local constructor to build this pagoda. Years after it was built, they noticed that the structural members seemed unstable and too small, therefore erupted this project. This research started by defining the scope and determining what kind of parameters are needed for analyzing the structure, hence the first task is to find out the loads that the current structure is carrying. To do so, the details of the pagoda structural members' dimensions are to be measured and quantified. Also, the embedded rebars are to be determined about their locations, dimensions and number of rebars. Ultimately, by using the principle of structural analysis and static studies, we can theoretically estimate the dead loads of the pagoda.

Fig. 1.1 Unfinished Pagoda at Putha-jedi temple

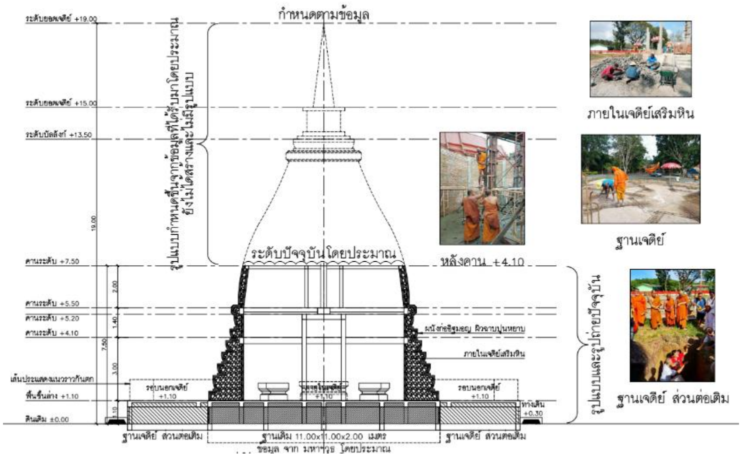

Fig. 1.2 Cross-section of Unfinished Pagoda

1.2 The dimension of the structural members

The unfinished pagoda generally consists of four levels of heights measuring from the ground to the bottom side of the beams: +4.10 m., +5.20/ +5.50 m. and +7.50 m. shown in Fig. 1.2 with each level having different configuration of structural member designs. Starting with the base of the pagoda which has 9 ground beams denoted as B2 and inside nonagon has another 8 ground beams in the shape of square denoted as B1. The weights carried by members B1 and B2 will be transferred to column C1 and C2. The details of each elevation are displayed in Fig 1.3, 1.4, 1.5 and 1.6.

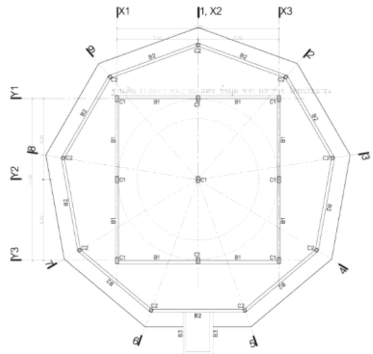

Fig 1.3 Top View +0.00 m.

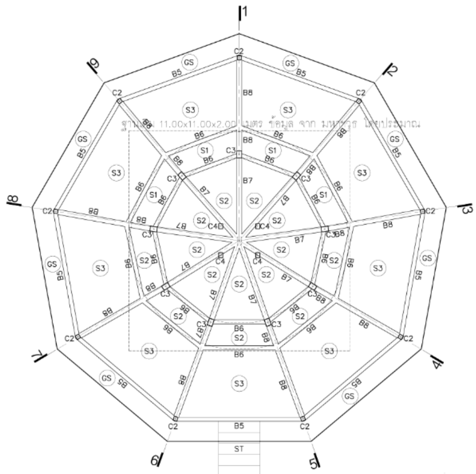

Fig 1.4 Top View +4.10

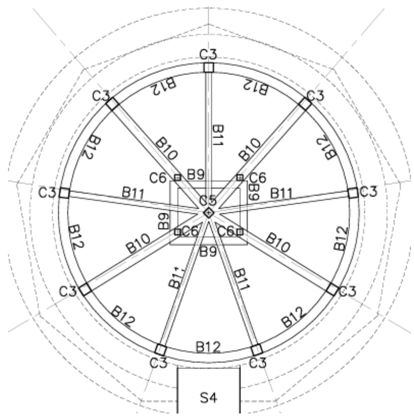

Fig 1.5 Top View +5.20/+5.50 m.

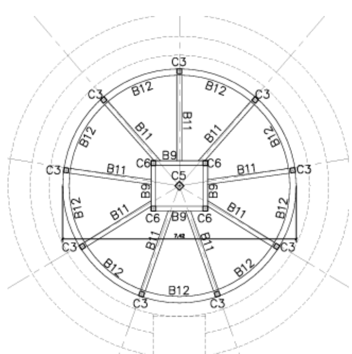

Fig 1.6 Top View +7.50 m.

1.3 Non-destructive testing

There are numerous methods of Non-Destructive testing (NDT), with each serves different purposes but first and foremost, we need to know what parameters we want to observe so we can choose appropriate testing methods to obtain those values which will be discussed in this paper. Moreover, it is crucial for engineers to know the physics behind each method before analyzing any structures so that we can understand what variables can affect the acquired values and why the number comes out as it is, hence, reliable results may be obtained. Some of the techniques are discussed in the following sections.

1.3.1 Scmidt hammer test

Rebound hammer test or Schmidt hammer test [1] comprises a spring-controlled mass sliding on a plunger within the tubular housing. When the plunger is pressed perpendicular against the concrete surface, a spring-controlled mass strikes the surface, and the rebound distance is measured, providing an indication of surface hardness. The measured value is known as Rebound Number or rebound index. Concrete with lower strength and stiffness tends to absorb more energy, resulting in a lower rebound number. This method can also be used to evaluate uniformity and can be correlated with the quality of concrete in accordance with standard specifications. However, there are some circumstances that need to be considered such as the concrete surface must be smooth, dry and clean which a grinding wheel or stone can be used to even out the surface before conducting the rebound hammer test.

1.3.2 Ultrasonic Pulse Velocity

Ultrasonic Pulse Velocity (UPV) [2] which measures the time taken or speed of ultrasonic pulse sent by a transducer, to pass through the specimen. This method usually requires a transducer, clock, oscillation circuit, and power source. Not only can it provide information about the homogeneity of the concrete but also can be used to correlate with the compressive strength of the concrete as well as Schmidt hammer test.

1.3.3 Ferro scan

Ferro scan and radar-based detection [3]. In the reinforced concrete evaluation, it is important to observe the location of reinforcement in the concrete structure. Ferro scan and radar technologies can provide information about their positions, diameter and dept of coverage. Also, other elements such as cables, tendons, conduits etc., can use these methods to find out their locations. The scanner device uses the principle of magnetic induction, a magnetic field is generated and analyzed in each movement and any distortion of the magnetic field may indicate the location of the reinforcing steel bars. The accuracy of the readings is dependent on certain conditions.

2. Methodology

From the on-site inspection, the measurement of the structural members details was quantified as well as the reinforcing rebars details by using the technique of radar scanning or Ferro scan. Next, the method of Schmidt hammer test is implemented to obtained the average compressive strength of concrete, denoted as fc'.

2.1 Concrete compressive strength from NDT

The Schmidt hammer test was implemented to obtained the average rebound numbers then they are translated into estimated fc' for cubic shape. However, we want the minimum fc' to determine the limit state of concrete so it is converted into fc' for cylindrical shape by multiplying with 0.8 [5] as it typically has lower fc'.

Location	Number	Average Rebound Number	Approximate Fc' for cubic ksc	Fc' cylinder ksc
Column 4 ต้น ในเจดีย์	1	31.6	320	256
	2	40.6	500	400
	3	28.4	282	225.6
	4	41.3	510	408
	Avg			322.4
Beam รอบนอกทางเดินเจดีย์	1	28.1	280	224
	2	28.8	290	232
	3	19.67	100	80
	4	25.1	225	180
	5	26.9	250	200
	Avg			183.2
Column หน้าทางเข้า	1	28.9	298	238.4
	2	43.4	543	434.4
	Avg			336.4
Column รอบเจดีย์	1	45.1	580	464
	2	36.7	410	328
	3	31.5	340	272
	4	30.8	318	254.4
	5	32	320	256
	6	37.9	442	353.6
	7	29.9	490	392
	8	27.4	485	388
	9	33.4	363	290.4
	Avg			333.2

Total avg 293.8 cylinder ksc

Table 1 Average Compressive Strength of Concrete by Schmidt Hammer

From Table 1, the minimum fc' for cylindrical shape is 183.2 ksc and the total average fc' is 293.8 ksc cylinder. Note that this method has high uncertainty [2] so usually another NDT is done to increase the credibility of the parameter. Supposedly, Ultrasonic Pulse velocity method (UVP) was to be implemented but due to the time limitation, coring the concrete specimen was a better option as it is more reliable [6] and easier to calibrate.

2.2 *Compressive strength from coring specimens*

The extracted cylindrical concrete specimens were brought back to Thammasat University, Civil engineering laboratory to test for concrete compressive strength (fc'). 7 samples were collected from different locations with the details as followed:

Table 2 Coring test result

Sample no.	Diameter (cm)	Height (cm)	H/D	Load (Kg)	Adjusted Fc' (ksc)
1.	4.31	8.92	2.07	1838	137
2.	4.31	8.72	2.02	2000	149
3.	4.31	6.59	1.53	1790	133
4.	4.31	8.45	1.96	1846	138
5.	4.31	9.04	2.10	1968	147
6.	4.31	5.70	1.32	1442	107
7.	4.31	8.94	2.07	2180	162

From Table 2, the average adjusted fc' is 135 ksc and comparing with the Schmidt hammer test result, it appeared to be lower hence the value that will be used for the calculation is referenced from the coring test instead as to assumed the concrete could only sustain the at the minimum.

2.3 *Difference between Schmidt hammer method and coring method*

The major difference between these two methods is that coring is considered as destructive testing that involve removing a concrete core, while Schmidt hammer is non-destructive, in-situ test. Both methods are used to assess the concrete strength, however the accuracy of each method is different. As the Schmidt hammer can quickly estimate fc', on the other hand, coring method takes more time and require more tools to calibrate the result. In spite of time-consumption, coring is much more reliable as it directly measures the fc'.

2.4 *Dimension of Beams and Columns*

After the site inspection, the dimensions of the cross-section of each beam and column are measured and quantified. Using the technique of Ferro scan to acquire the reinforcing rebars details which all will be presented in Fig 2.1,2.2,2.3 for beams and Fig 2.4,2.5 for columns.

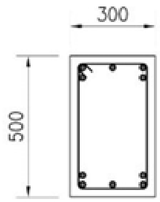

Fig 2.1 Cross-section of B1-5, B7-8

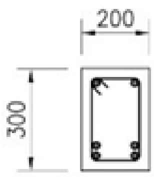

Fig 2.2 Cross-section of B6

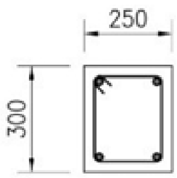

Fig 2.3 Cross-section of B9-12

Table 3 Beam details

Type	B1-5, B7-8	B6	B9,B11	B10,B12
size	300x500	200x300	200x300	200x300
Top bar	5DB12	2DB12	2DB12	2DB12
Bottom bar	4DB16+1DB12	4DB12	2DB12	4DB12
Stirrup	RB6@150	RB6@150	RB6@200	RB6@150

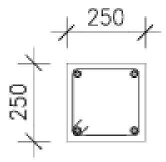

Fig 2.4 Cross-section of C1, C2, C3

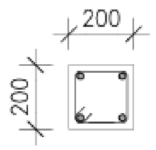

Fig 2.5 Cross-section of C4, C5, C6

Table 4 Columns details

Column details at each elevation			
		C1,C2,C3	C4,C5,C6
Elev. +5.10	Rebar	4DB16	4DB12
	Stirrup	RB6@200	RB6@150
Elev. +1.10	Rebar	4DB16	4DB12
	Stirrup	RB6@200	RB6@150
Foundation	Rebar	4DB16	4DB12
	Stirrup	RB6@200	RB6@150

3. Results and Discussion

After all the acquired parameters are determined, the results are calculated by using a program ETABS [4], compared between loads and resistances which essentially are the stiffness of each stress. If the resistance is greater than the load so the member is able to withstand that load however, if not then the structure has to be re-built, strengthened or redesigned. The data of beams and columns' structural loads compared to the structural resistance in Fig 3.1-3.10 and Table 5-8. Lastly, the satisfied and unsatisfied members are accounted and summarized in Table 8. Regardless on how to strengthen the members or re-build the pagoda, the unsatisfied members shall be strengthening, to have higher resistance to sustain the structural loads and the satisfied members may be kept.

Table 5 Moment and Shear in B1-5, B7-8

Beam no.1-5, no.7-8	Structural load Q			Resistance load R		
	Start	Mid	End	Start	Mid	End
Moment	- 4062	26575	-37605	-12250	12250	12250
Shear	9202	33323	34280	10500	10500	10500

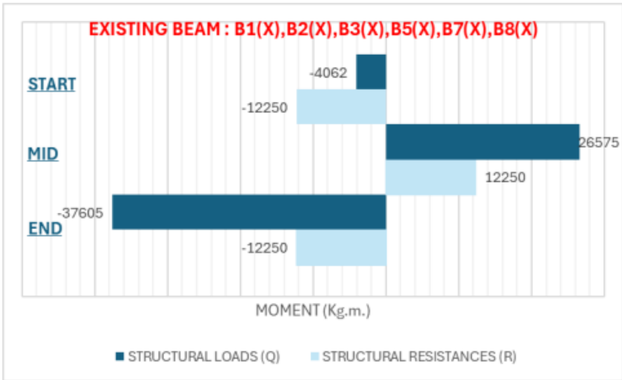

Fig 3.1 Comparison of Moment in B1-5, B7-8

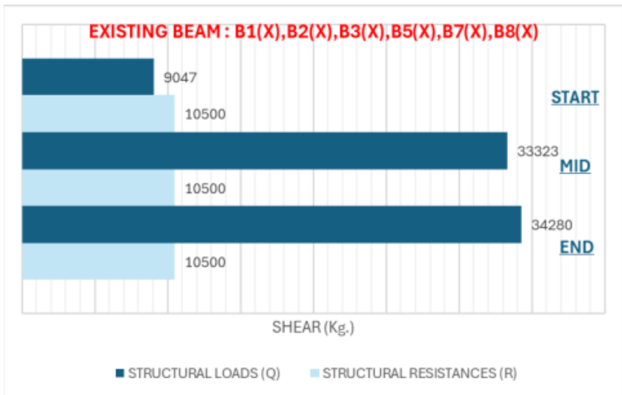

Fig 3.2 Comparison of Shear in B1-5, B7-8

Table 6 Moment and Shear in B6

Beam no.6	Structural load Q			Resistance load R		
	Start	Mid	End	Start	Mid	End
Moment	-3840	2164	1877	-2600	2600	2600
Shear	3797	1113	1014	4800	4800	4800

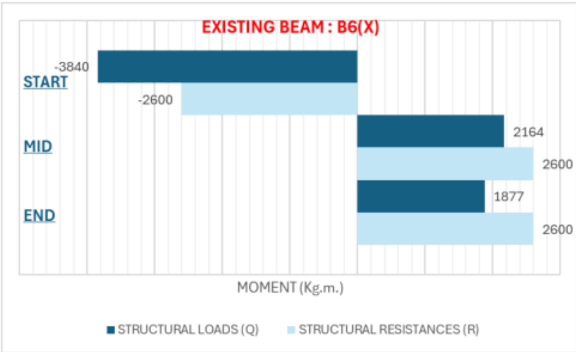

Fig 3.3 Comparison of Moment in B6

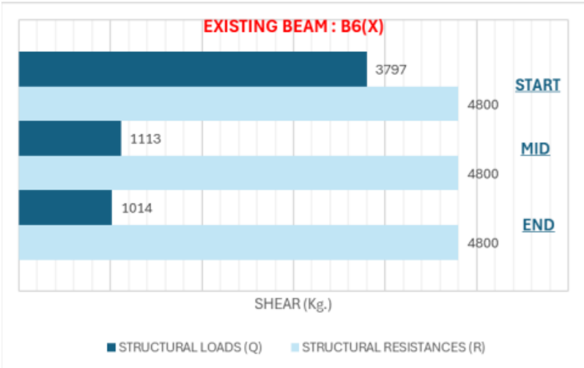

Fig 3.4 Comparison of Shear in B6

Table 7 Moment and Shear in B9 and B11

Beam no.9, no.11	Structural load Q			Resistance load R		
	Start	Mid	End	Start	Mid	End
Moment	5855	-2931	-744	2000	-2000	2000
Shear	1816	2780	63	5700	5700	5700

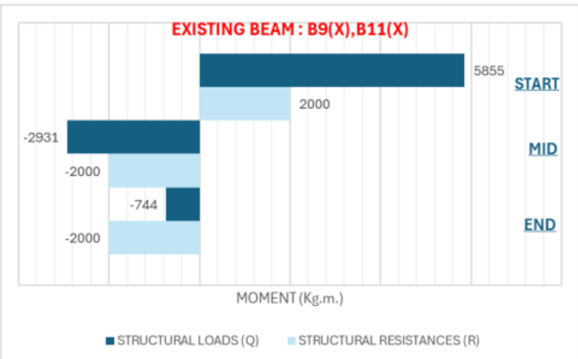

Fig 3.5 Comparison of Moment in B9 and B11

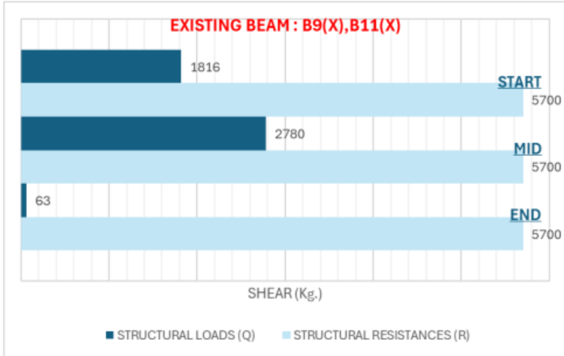

Fig 3.6 Comparison of Shear in B9 and B11

Table 8 Moment and Shear in B10 and B12

Beam no.10, no.12	Structural load Q			Resistance load R		
	Start	Mid	End	Start	Mid	End
Moment	-793	-3909	4833	-2700	-2700	2700
Shear	397	2894	1904	5500	5500	5500

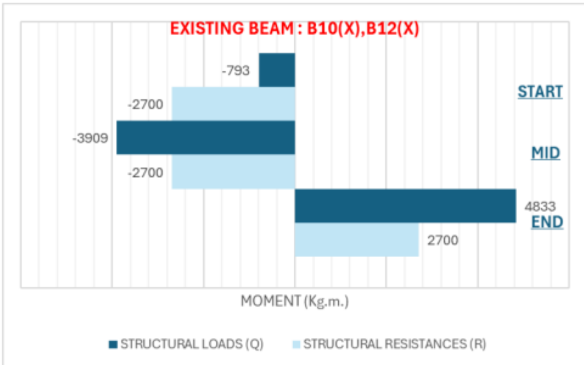

Fig 3.7 Comparison of Moment in B10 and B12

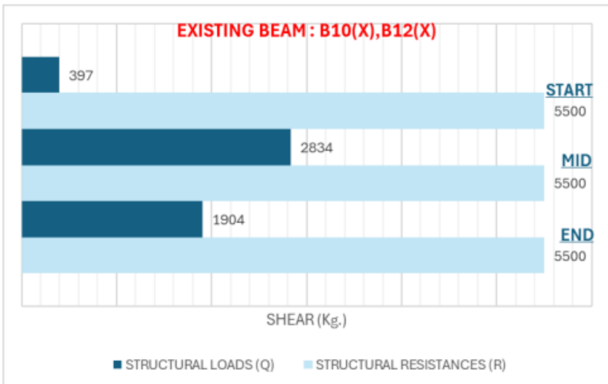

Fig 3.8 Comparison of Shear in B10 and B12

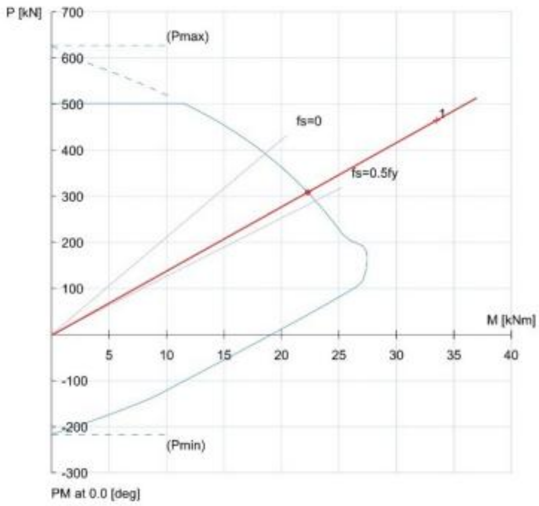

COLUMN NO.		STRUCTURAL LOADS (Q)	STRUCTURAL RESISTANCES (R)
C1X,C2X,C3X	Axial Load (KN.)	465.1	310
	M (KN.m.)	33.5	22

Fig 3.9 Interaction Diagram of Columns C1, C2, C3

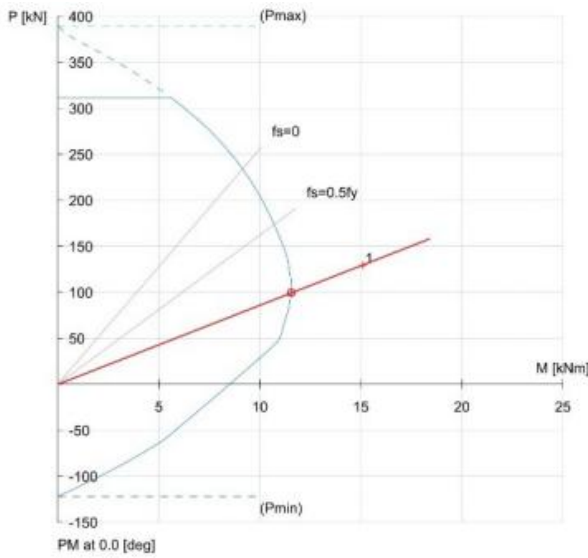

COLUMN NO.		STRUCTURAL LOADS (Q)	STRUCTURAL RESISTANCES (R)
C4X,C5X,C6X	Axial Load (KN.)	129.2	100
	M (KN.m.)	15.1	12

Fig 3.10 Interaction Diagram of Columns C4, C5, C6

Table 9 Summarized Results

Columns	Unsatisfied Q>R	Total	Beams	Unsatisfied Q>R	Total
C1	1	1	B1	6	8
C2	3	9	B2	0	9
C3	14	19	B3	0	3
C4	12	13	B5	1	9
C5	9	9	B6	4	18
C6	8	8	B7	8	9
			B8	0	9
			B9	12	12
			B10	6	8
			B11	8	10
			B12	9	36
		80%			92%

From Fig.3.2, shear loads exerted were triple the structural resistances but shear resistances in B6 shown in Fig.3.4, B10 and B12 in Fig 3.8 and of shear in B9 and B11 in Fig 3.6, have higher resistances to the structural loads. This shows the in consistencies and of loads applied. In term of moment, in almost every part (start/mid/end) of the members of all beams, they are not capable to withstand the moments; only a single part for example in Fig 3.5, only at the end of B9 and B11 has slightly higher moment resistance than the structural loads. To conclude, most beams are able to sustain shear forces but none could sustain moment forces

From Table 9, out of all 59 columns and 131 beams, only 12 columns and 77 beams have higher resistance than the structural loads. The properties of failure of the pagoda meaning that up to 80% of columns and 92% of beams were under designed theoretically. Both structure members make up for the total average fail rate of the whole structure to 86%. This value, however, does not speak for the entire structure as this paper did not speculate on the foundation work but only the superstructure. Nevertheless, it is safe to say that this structure built without referencing the principle of civil engineering cannot sustain the structural loads with the current design.

4. Conclusion

From the calibrated results, they showed that out of all columns, the probability of failure of columns and beams are 0.8 and 0.92 respectively. Hence there is a high risk of failure or perhaps collapse. Although there is a probability of survival about 0.2, it is expected that the pagoda will not have a long life-span and It will probably need constant maintenances in the long run. The results also illustrated that the designs did not take in account of safety factor. It is recommended by the related engineers that the structure should be re-designed or re-build rather than strengthening the current pagoda as this solution can be as expensive as building a stronger one.

Acknowledgement

I express my heartfelt gratitude to my assistance professor, Prof. Saharat. and his colleague, a licensed civil engineer, Mr. Kovit. Thank you for your cooperation and guidance in completing this paper, without your patience and constant encouragement, I would not have been able to do it on my own.

References

[1] Onur Yücel (2015). Ferroscan and radar-based detection and analysis technologies for non-destructive testing. *HITI Corporation, Ankara, Turkey.* SMAR 2015 Third Conference on Smart Monitoring, Assessment and Rehabilitation of Civil Structures.

[2] Irpan Hidayat, Audry Farrel Shang Rahardhani, Gabriellela Aprilyanthi Suhardjo. Utilizing hammer tests and ultrasonic pulse velocity to ascertain the compressive strength of concrete. The 7th International Conference on Eco Engineering Development 2023 (ICEED 2023)

[3] Miguel C. S. Nepomuceno and Luís F. A. Bernardo. Evaluation of Self-Compacting Concrete Strength. Appl. Sci. 2019, 9, 5109

[4] 2011, American Concrete Institute (ACI 318-11), Farmington Hills, MI.

[5] Reddy, Dr & Seshagiri Rao, Mv & Shrihariis, Dr. (2019). Strength Conversion Factors for Concrete Based On Specimen Geometry, Aggregate Size and Direction of Loading. International Journal of Recent Technology and Engineering (IJRTE). 8. 2125-2130. 10.35940/ijrte.B2336.078219.

[6] Jukka Haavisto, Ari Husso and Anssi Laaksonen. Compressive strength of core specimens drilled from concrete test cylinders. Structural Concrete. 2021;22 (Suppl. 1): E683–E695.